ISSN : 0974-7419 Volume 15 Issue 12

Analytical CHEMISTRY

An Indian Journal

Full Paper

ACAIJ, 15(12) 2015 [514-525]

# The supramolecular complex formation between erichrome blue black R and P-sulfonated calixarenes: A spectrofluorimetric study on their inclusion interaction

**Cheng-Xuan Hao, Hong Tian, Hai-Long Liu, Li-Ming Du*, Qing-Hua Zhao, Xiao-Hui Guo, Yun-Long Fu**

**Analytical and Testing Center, Shanxi Normal University, Linfen, 041004, (P.R.CHINA)**
**E-mail: lmd@dns.sxnu.edu.cn**

## ABSTRACT

The fluorescent characteristic of chrome blue black R(EBBR) and its ability of binding to p-sulfonated calix[n]arene (SCnA, n=4,6,8) as a guest moleculehave been studied by fluorescence methods and a variety of techniques. According to the fluorescence spectra, it was found that EBBR might have different conformations under different conditions of acidity, which was validated by UV spectrophotometer. The stability constants were determined at different temperatures and different pH by spectrofluorometry titrations, the thermodynamic parameters of the obtained complex were evaluated and the impact of both kinds of molecules during the inclusion were measured quantitatively. The results show that the binding constants increase when the size of calixarene cavity becomes enlargedÿindicating that the larger host cavity can accommodate the guest molecule better. The impact of ionic strength on the system were further investigated. In addition, $^{1}$H NMR studies were carried out to explore the mechanisms of their interaction. It showed that EBBR partly penetrated into the cavity of p-sulfonated calix[n]arene. We found that the assumptions about steric hindrance between the sulfonic acid groups are established by molecular simulation of clathrate. The data calculated by molecular simulation is consistent with the findings obtained by fluorescence and $^{1}$H NMR. 

## KEYWORDS

Chrome blue black R;
P-sulfonated calix[n]arene;
Spectrofluorometry;
Thermodynamic parameters.

## INTRODUCTION

Recently, non-covalent intermolecular interactions have been found to play a major role in biological chemistry as well as in supramolecular chemistry[1] But the poor solubility or stability of some moleculars limits their applications[2]. Calixarenes, composed of phenolic units linked by methylene groups, have been described as "macrocycles with (almost) unlimited possibilities".[3] Because of their cavities were easy to be modified, a class of variable calixarene derivatives called p-sulfonated calixarenes were synthesized.[4] Given its three-dimensional and flexible π-rich cavities with numerous binding sites, low toxicity and great water solubility,[5] the SCnA family is emerging as the research

focus by many chemists, pharmacologists and biologists.[6-8] Sulfonated calixarenes are able to be complexed with a number of guest molecules and especially, a number of different objects, including inorganic cations,[9,10] organic ammonium cations,[11,12] neutral molecules,[13] dyes,[14-15] the native amino acids,[6] proteins[16] as well as drug molecules,[17-20] which have recently been published. However, compared to crown ethers or cyclodextrins which have been widely used in the chemical synthesis, chemical analysis and pharmaceutical industry, the research about water-soluble sulfonated calixarenes are still very limited. In particular, it was reported by only a few literatures that guest molecules interacted with different calixarenes showing natural fluorescence characteristics.

Chrome blue black R is a common dye and widely used as an organic ligands in the determination of metal ions. It can be used to determine the concentration of copper, calcium, iron irons in aqueous solution[21,22] and biological samples such as amino acids and proteins, etc.[23] It can also be utilized to take preparation of complex indicator. Eriochrome Blue Black R can be dissolved in an aqueous solution and compared to many other organic dyes,it has high fluorescence intensity. There is - N = N - linked with naphthalene rings on both sides in molecule structure and its size is close to the size of the calixarene cavity.

In this study, we respectively investigated the interaction between EBBR and SCnA (n = 4, 6, 8) (their structures shown in Figure 1) in aqueous solution by fluorescence spectrophotometric titration. With the increase of the pore structure of SCnA, the quenching of fluorescence intensity of EBBR gradually increases. We also investigated the effects of temperature and pH on the stability constant of inclusion complexes, measured their thermodynamic properties and obtained the thermodynamic parameters related to inclusion. Further, molecular modeling and $^1$H NMR studies were carried out to determine the possible mechanisms for the binding reaction and the impact of surfactant and common impurity ions on EBBR-SCnA were also detected. We found there was a strong interaction between EBBR and SCnA with a strong anti-interference ability. Due to the high sensitivity, good selectivity and simple instrument of this method, it is an effective analytical tool and suitable for the study of interaction between the fluorescent guest molecules and sulfonated calixarenes. Our data provides an approach to find potential calixarene fluorescent probes and expands the applications of water-soluble calixarenes in molecular recognition and analytical chemistry.

## EXPERIMENTAL

### Chemicals

All reagents were commercially available and used with analytical reagent grade or the best grade. During the experiment double-distilled water was used without impurities detected by fluorescence. EBBR used in the experiment were obtained from China Tianjin Chemical Reagent Factory. SCnA

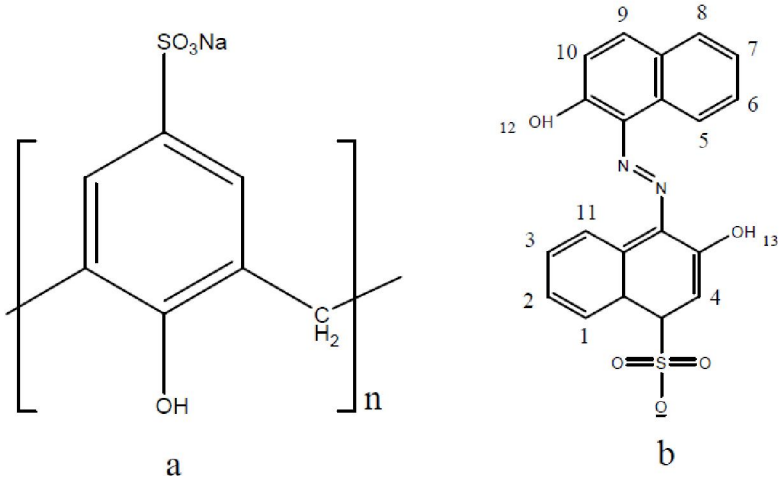


**Figure 1 : The structure of *p*-sulfonated calix[*n*]arene (*n*=4,6,8) and EBBR**

Full Paper

(n=4,6,8) were purchased for TCI Chemical Industry Co., Ltd (Shanghai, China). EBBR and SCnA stock solution ($1.0\times10^{-3}$ mol $L^{-1}$) were prepared respectively in 100 mL volumetric flasks. Working solutions were made by dilution of the stock solution as needed. All standard stock solutions were kept stable for several weeks at room temperature and working solution was freshly prepared. A Britton-Robinson (BR) buffer solution (pH 2.00–11.00) was prepared using 0.04 mol $L^{-1}$ boric acid, acetic acid and phosphoric acid, and subsequently was adjusted to accurate pH values by adding 0.2 mol $L^{-1}$ sodium hydroxide.

### Apparatus

Fluorescence spectra were obtained with Cary Eclipse Fluorescence spectrofluorometer (Agilent Technologies) using an excitation and emission wavelength at 224 nm and 357 nm respectively. The UV absorption experiments were performed on Cary 300 Scan UV-visible spectrophotometer(Varian Ltd.). All measurements were set up at room temperature about 20.0 ± 0.5 °C. The pH values were adjusted with a pHS-3TC digital precision pH meter (Shanghai, China). During the experiment influenced by temperature, the temperatures were controlled by using a thermostated cell holder and a thermostatically controlled water bath. $^1$H NMR spectra were measured and recorded on a Bruker DRX-600MHz spectrometer (Switzerland) using $D_2O$ as solvent. Molecular modeling were calculated and optimized at the B3LYP/6-31G (d) level of density functional theory through the Gaussian 03 program.

### Experimental procedure

Totally 1.0 mL EBBR solution ($3.0\times10^{-5}$ mol $L^{-1}$) was transferred into a 10 mL volumetric flask, following by addition of an appropriate amount of $1.0\times10^{-4}$ mol $L^{-1}$ SCnA. The pH was accurately controlled by the introduction of 1.0 mL of Britton-Robinson buffer solutions. The combined solution was diluted to the final volume with distilled water, shaken thoroughly, and then equilibrated for 15 min at room temperature. Subsequently absorption and emission fluorescence intensity were meassured.

## RESULTS AND DISCUSSION

### Spectral properties of EBBR

The presence of EBBR are closely related to the medium acidity. In this study, EBBR fluorescence peaks were measured in different acidity. The results shown below in Figure 2

The relatively strong fluorescence peak of EBBR was shown at 356nm in an aqueous solution of pH=2, and while pH=10, the peak is at 420nm. Further, when EBBR exists in the solution under a dynamic equilibrium of system (pH between 3-10), the fluo-

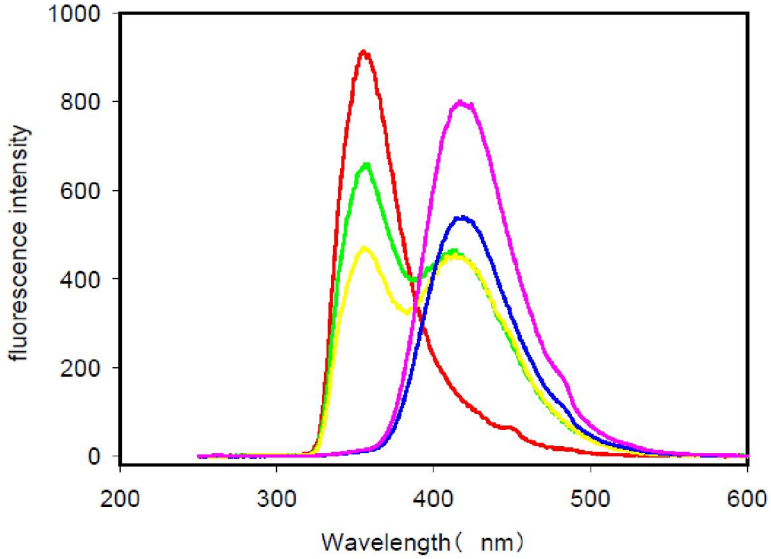


**Figure 2 : The fluorescence spectra of EBBR (3×10-6 mol L-1) in different pH: (Red)pH=2; (Green) pH=3; (Yellow) pH=9; (Blue)pH=10; (Pink) pH=11**

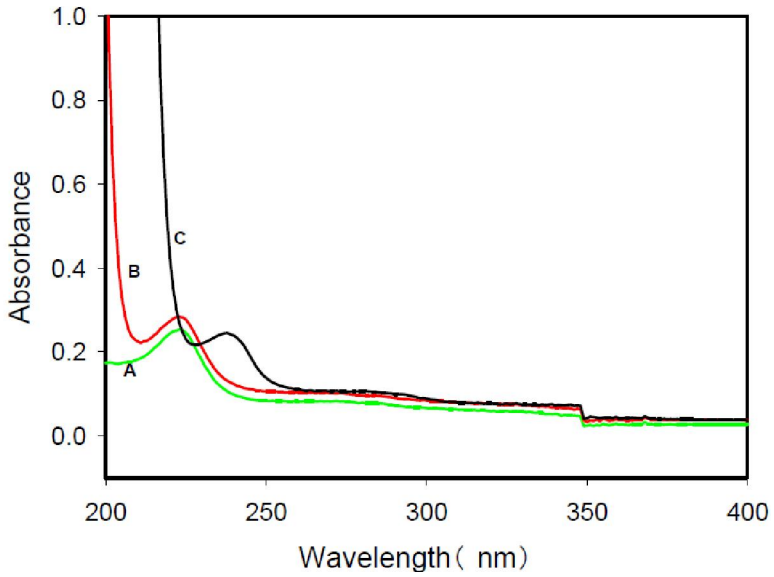


**Figure 3 : EBBR absorbance in different pH (A) PH=7 (B) PH=2 (C) PH=11**

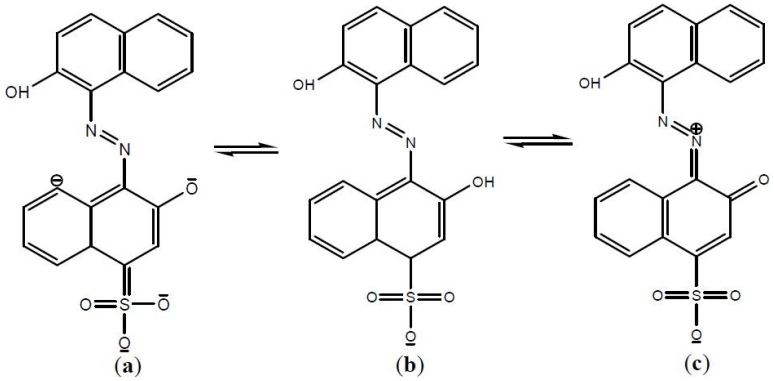


**Figure 4 : The most probable species of Eriochrome Blue Black R at low- and high pH values.in Britton-Robinson buffer solutions. (a) Molecular conformation in alkaline solution (b) Molecular conformation in neutral solution (c) Molecular conformation in acidic solution**

rescence peaks appear at both 356nm and 420nm and the intensity of peak changes with the increase of pH values. The fluorescence intensity at 356nm gradually decreases while the intensity at 420nm gradually increases. Thus, we propose that EBBR show the different fluorescence peaks at different pH values due to its protonation and tautomerism. To test this hypothesis, the absorbance of EBBR in acidic, neutral and alkaline conditions was measured by UV-visible spectrophotometer (Figure 3).

UV absorption of EBBR in neutral (A), acidic (B) and alkaline (C) conditions is respectively detected. Under the acidic condition, EBBR absorbance increases, showing the increased conjugation effects. Under the alkaline condition, the maximum absorption shifts to the red, indicating the variable conjugate structure length and increased conjugate effects too. This findings are consistent with assumptions that EBBR's different conformations exist in different acidity solutions proposed by Silvina Pirillo[24] and others (Figure 4).

## The formation process of the complex

When SCnA (n = 4, 6, 8) was added, EBBR ($3.0 \times 10^{-6}$ mol $L^{-1}$) showed a strong fluorescence quenching. EBBR-SCnA complex formation was confirmed by fluorescence spectra analysis. With the addition of $1.0 \times 10^{-5}$ mol $L^{-1}$SCnA, EBBR fluorescence intensity significantly goes down and the orderly reduction of fluorescence intensity is consistent with the size of calixarene ring in order, namely, SC4A <SC6A <SC8A. Since EBBR showed different fluorescence spectra under various acid conditions, the fluorescence intensity of EBBR-SCnA was measured

Full Paper

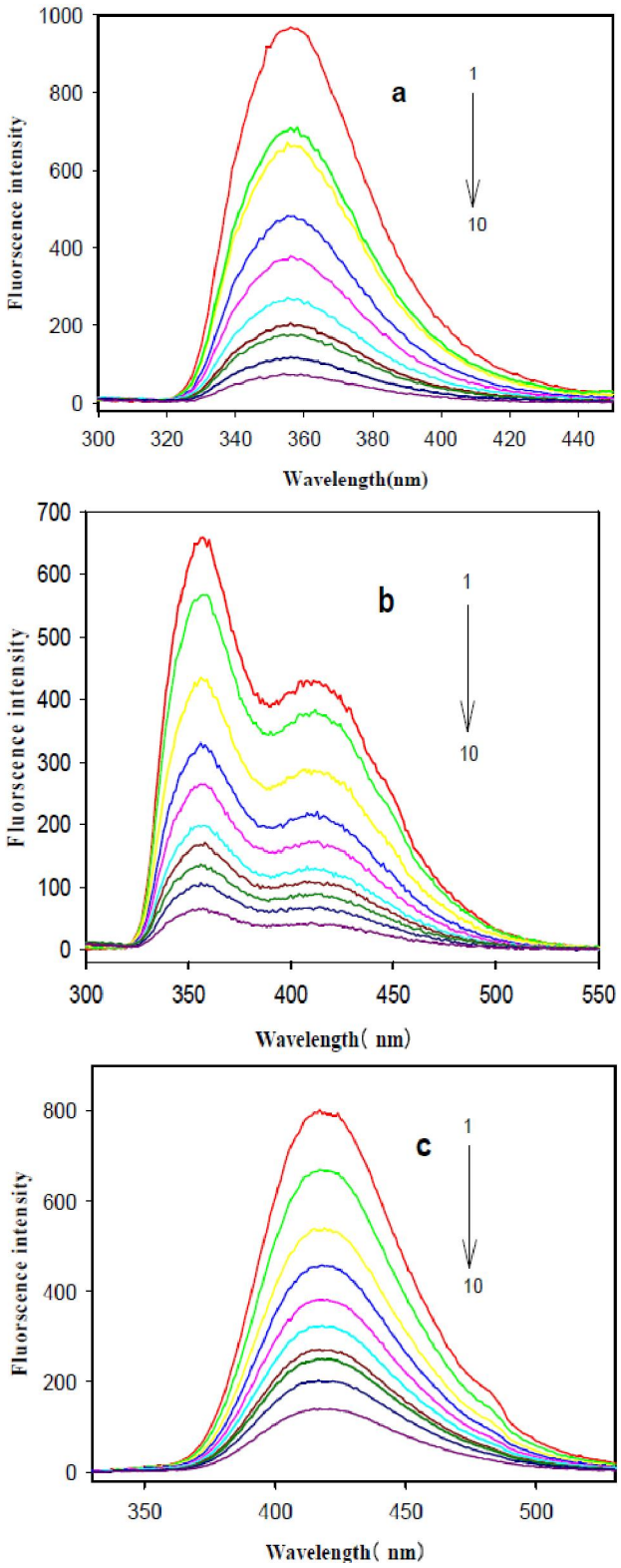


**Figure 5 : The fluorescence spectra of EBBR in different concentrations of SC8A in Britton-Robinson buffer solutions at 293K and Figure a、b、c correspond to pH=1,pH=7,pH=11. The concentrations of SC8A ($10^{-5}$ mol $L^{-1}$): (1) 0; (2) 0.1; (3) 0.3; (4) 0.5; (5) 0.7; (6) 0.9; (7) 1.1; (8) 1.3; (9)1.5; (10)2.0; $C_{EBBR}$=3.0×$10^{-6}$mol $L^{-1}$**

under the condition of pH = 6, pH = 7, pH = 11 accordingly. The measurement of the representative EBBR-SC8A system was shown in Figure 5 and EBBR-SC4A or EBBR-SC6A display the same trend but the less quenching. The significant reduction of fluorescence intensity demonstrated the formation of EBBR-SCnA complex. Moreover, we further investigated the effects of SCnA concentration on the fluorescence intensity of EBBR-SCnA complex. EBBR concentration was maintained constant at 3.0 × $10^{-6}$ mol $L^{-1}$ and we gradually increased the concentration of SCnA. Our results show that when SC4A, SC6A, SC8A concentrations were respectively more than 6.0 × $10^{-5}$mol $L^{-1}$, 4.0 × $10^{-5}$ mol $L^{-1}$, 3.0 × $10^{-5}$mol $L^{-1}$, the fluorescence intensity of EBBR gradually maintain steady, demonstrating that the solution has reached the equilibrium condition.

## Stoichiometry and inclusion constant determination

The inclusion capacity of a host in relation to specific guest was described as Inclusion formation constant (K). Under the current experimental conditions, It was presented as follows: when EBBR and SCnA was complexed at the ratio of 1:1, K could be obtained by the following calculation:

$$EBBR + SCnA \quad EBBR - SCnA \qquad (1)$$

$$K = \frac{C_{\text{EBBR-SC}n\text{A}}}{C_{\text{EBBR}} \times C_{\text{SC}n\text{A}}} \qquad (2)$$

where $C_{EBBR}$, $C_{SCnA}$, and $C_{EBBR-SCnA}$ are presented as equilibrium concentrations. So K value can be determined by the typical double reciprocal or Benesi – Hildebrand plots.[25]

$$\frac{1}{F - F_0} = \frac{1}{(F_\infty - F_0)KC_{\text{SC}n\text{A}}} + \frac{1}{F_\infty - F_0} \qquad (3)$$

Where F is the observed fluorescence intensity when each corresponding SCnA concentration was tested, $F_0$ is the fluorescence intensity of EBBR without the addition of SCnA and F∞ is the enhancement once all EBBR (100% EBBR) is complexed.

When $1/(F–F_0)$ was plotted against $1/C_{SCnA}$, A good linear change was obtained, indicating the existence of a 1:1 complex ($R^2 > 0.99$, see Figure 6). The remarkable association constants for these com-

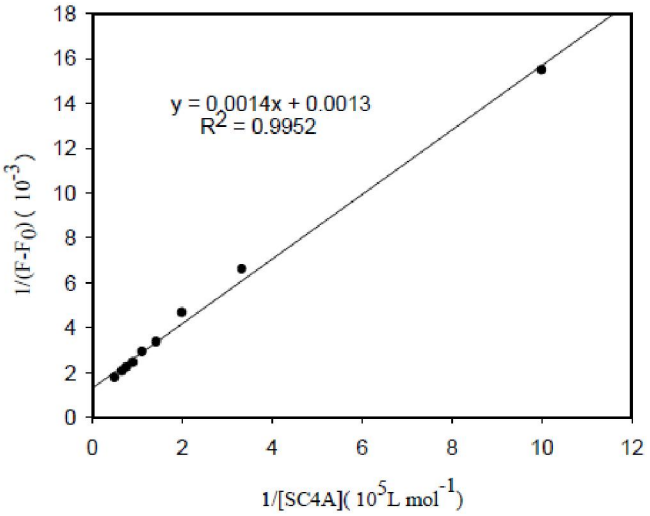


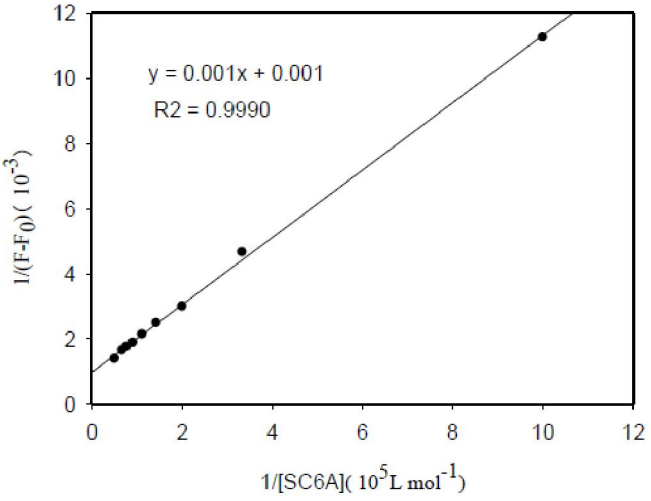


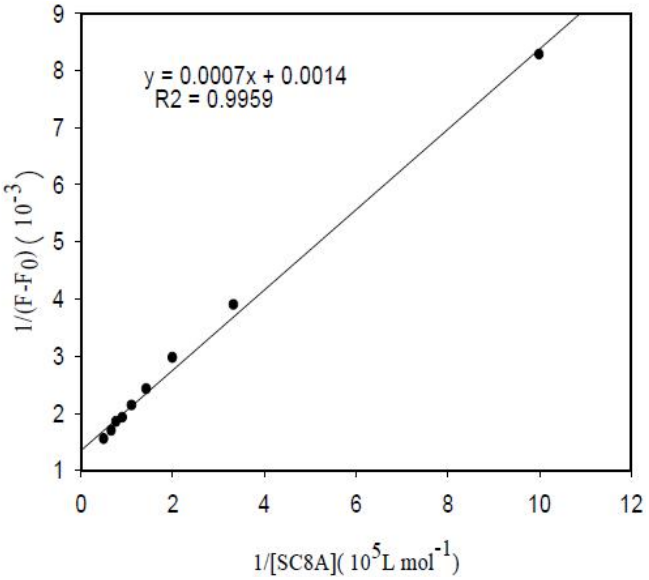


**Figure 6 : Plot of $1/(F–F_0)$ versus 1/ [SCnA] of SCnA–EBBR complex**

plexes were obtained from the ratio of the intercept to the slope of the corresponding lines which can be calculated as $0.93\times10^5$ L mol$^{-1}$, $1.00 \times 10^5$ L mol$^{-1}$, and $2.00 \times 10^5$ L mol$^{-1}$ in presence of SC4A, SC6A and SC8A, respectively. The bigger inclusion constants demonstrate much stronger interaction of EBBR with SCnA and monotonically they raise with the increasing number of phenolic units in the calixarene ring.

To further evaluate the stoichiometry for EBBR-SCnA inclusion complex, Job's plot was generated which was shown in Figure 7. The peak of the curve was apparently at a mol fraction of 0.5, verifying that the assembly of 1:1 ratio host–guest complex was formed in aqueous solution[26]. This finding is in agreement with the double reciprocal plot.

## Thermodynamic parameters of inclusion complexation

To elucidate the thermodynamic origins of the inclusion complex formation, the stability constants at various temperatures ranging from T = (283 to 313) K were observed by fluorescence spectra as shown in TABLE 1. If the enthalpy change (ΔH) did not alter significantly witinh the temperature range, then its value and that of entropy change (ΔS) can be determined according to the Van't Hoff equation[27]. Where R was the gas constant, the enthalpy change (ΔH) and the entropy change (ΔS) relevant to complex formation.

$$\ln K = -\frac{\Delta H}{RT} + \frac{\Delta S}{R} \qquad (4)$$

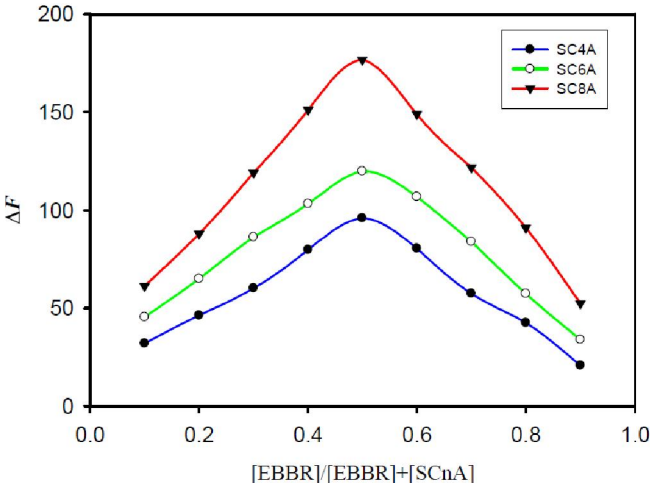


**Figure 7 : Job's plot for the complexation of EBBR with SC*n*A in Britton-Robinson buffer solution at 20°C. ([EBBR] + [SC*n*A]) = $3.0\times10^{-6}$ mol L$^{-1}$)**

Full Paper

**TABLE 1 : Complex stability constants (*K*) and thermodynamic parameters for 1:1 intermolecular complexation of EBBR with SC*n*A (*n*=4,6,8) in Britton-Robinson buffer solution at different temperature**

| | T(K) | K(L mol$^{-1}$) | H(kJ mol$^{-1}$) | ΔS(J/(mol K) $^{-1}$) | ΔG(kJ mol$^{-1}$) |
|---|---|---|---|---|---|
| | 283 | $0.71\times10^5$ | | | -26.28 |
| | 293 | $0.93\times10^5$ | | | -27.84 |
| SC4A | 298 | $1.04\times10^5$ | 17.88 | 156.05 | -28.62 |
| | 303 | $1.18\times10^5$ | | | -29.41 |
| | 313 | $1.46\times10^5$ | | | -30.97 |
| | 283 | $0.75\times10^5$ | | | -26.41 |
| | 293 | $1.00\times10^5$ | | | -28.08 |
| SC6A | 298 | $1.18\times10^5$ | 20.87 | 167.09 | -28.92 |
| | 303 | $1.38\times10^5$ | | | -29.75 |
| | 313 | $1.72\times10^5$ | | | -31.43 |
| | 283 | $1.25\times10^5$ | | | -27.59 |
| | 293 | $2.00\times10^5$ | | | -29.78 |
| SC8A | 298 | $2.57\times10^5$ | 34.52 | 219.45 | -30.88 |
| | 303 | $3.30\times10^5$ | | | -31.98 |
| | 313 | $5.06\times10^5$ | | | -34.17 |

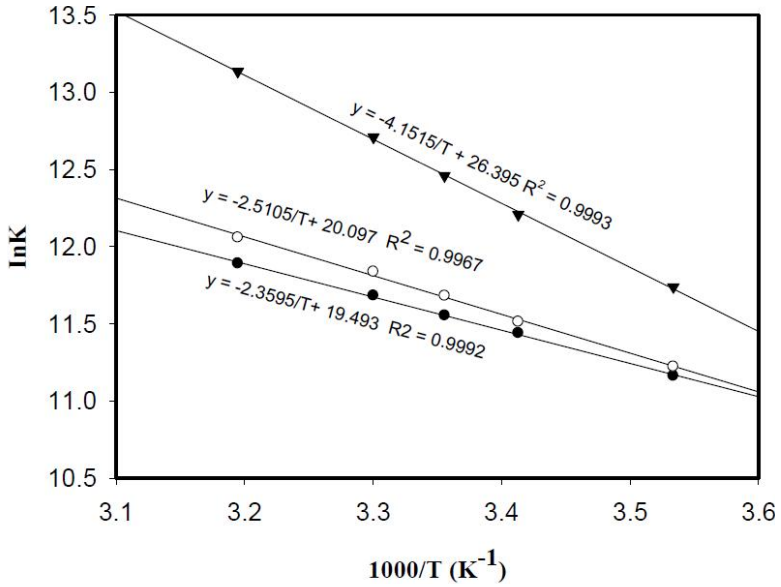


**Figure 8 : Van't Hoff plot, $C_{EBBR}=3.0\times10^{-6}$ mol L$^{-1}$**

A plot of ln K versus 1/T was linear within experimental error, which was shown in Figure 8. The value of the alterations in enthalpy and entropy could be acquired from the slopes and ordinates at the origin of the fitted lines, respectively. The free energy change (ΔG) was obtained from the following equation.

$$\Delta G = \Delta H - T\Delta S \quad (5)$$

As shown in TABLE 1, the negative sign for the free energy of EBBR-SCnA indicated that their interaction process was spontaneous. Enthalpy-entropy is positive indicating that the reaction is an endothermic reaction and is accompanied by a small amount of entropy loss. These results indicate that the entropic driving force facilitates the formation of EBBR–SCnA complex. The enthalpy change results from several factors, one of the most important being the nature of the intermolecular host–guest in-

teractions[28]. In our study, the major contributions probably come from the hydrophobic interactions with some contributions of van der Waals interactions and hydrogen bond. At the same time, the conformation change and the desolvation effect contributed to the entropic changes. Entropy change was closely related to the entropic gain from rearrangement of water molecules originally surrounding the host and guest molecules, and the Entropy loss due to restricted mobility of the guest molecule predominates in the case of complexation with calix[n]arene-p-sulfonates[29]. Higher temperature was advantageous to the formation of inclusion complexes, but the fluorescence intensity of EBBR in high temperature is unstable. Therefore, the present experiment was conducted at room temperature.

## Influence of ionic strength

It was well known that calixarenes and their derivatives can form non-covalent inclusion complexes with various guest molecules of suitable size and characteristics with the aid of electrostatic interaction, cation–π interactions, hydrogen bonding, van der Waals, hydropHobic interactions, and so on[30]. In order to probe the main driving force for the inclusion of EBBR by SCnA, the effect of NaCl ionic strength on the inclusion process was examined. Our findings show the effect of ionic strength on the fluorescence quenching intensity of EBBR-SCnA system (Figure 9). Apparently, NaCl ionic strength has no strong effect on the inclusion process, and the corresponding inclusion constants obtained by calculation have no obvious changes,showing that the main driving force for inclusion of EBBR by SCnA is not electrostatic interaction. The result is consistent with the investigation of the main force between the p-sulfonatocalix[4] arene and methiocarb reported by Xue-Ping Ding et al.[31] Therefore, the hydrophobic interaction and the size/shape fitting effect were considered to play the main roles during the formation of host–guest complex. This was different from the lomefloxacin-p-sulfonated calix[4]arene system, where electrostatic interaction was thought to play important part in the inclusion process.

## Effect of pH

As mentioned above, EBRR is apt to be affected

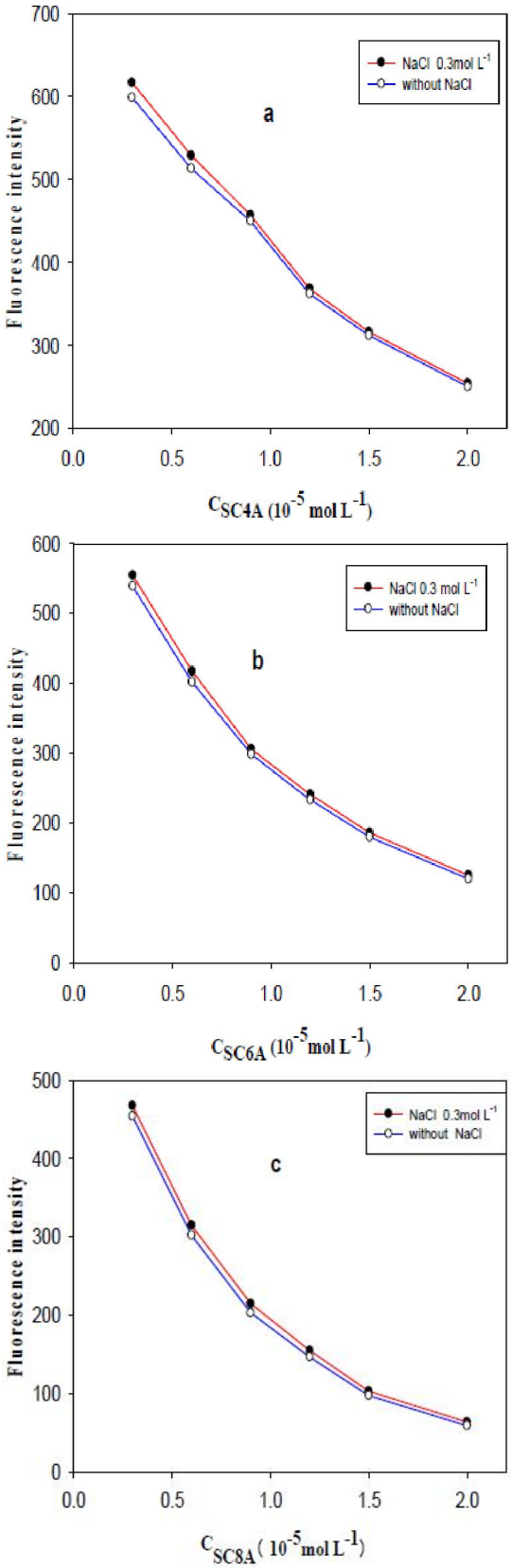


**Figure 9 : Influence of NaCl ionic strength on the fluorescence quenching intensity of SC6A–EBBR system, $C_{SC6A}$ = 1.0×10$^{-5}$ mol L$^{-1}$, $C_{EBBR}$= 3.0×10$^{-6}$ mol L$^{-1}$.**

Full Paper

**TABLE 2 : Complex association constants for 1:1 intermolecular complexation of EBBR with SCnA at different pH**

| | | pH | | | | | | | | | |
|---|---|---|---|---|---|---|---|---|---|---|---|
| | | 2 | 3 | 4 | 5 | 6 | 7 | 8 | 9 | 10 | 11 |
| | | m=1:1 | m=1:1 | m=1:1 | m=1:1 | m=1:1 | m=1:1 | m=1:1 | m=1:1 | m=1:1 | m=1:1 |
| SC4A | K | $0.444\times10^5$ | $0.611\times10^5$ | $0.632\times10^5$ | $0.875\times10^5$ | $0.929\times10^5$ | $0.588\times10^5$ | $0.550\times10^5$ | $0.074\times10^5$ | $0.267\times10^5$ | $0.289\times10^5$ |
| | $R^2$ | 0.998 | 0.996 | 0.996 | 0.993 | 0.997 | 0.995 | 0.999 | 0.986 | 0.995 | 0.991 |
| SC6A | K | $0.462\times10^5$ | $0.667\times10^5$ | $0.700\times10^5$ | $0.818\times10^5$ | $0.667\times10^5$ | $1.000\times10^5$ | $0.76\times10^5$ | $0.143\times10^5$ | $0.876\times10^5$ | $0.967\times10^5$ |
| | $R^2$ | 0.996 | 0.999 | 0.996 | 0.999 | 0.999 | 0.992 | 0.997 | 0.993 | 0.996 | 0.996 |
| SC8A | K | $0.818\times10^5$ | $1.143\times10^5$ | $1.143\times10^5$ | $1.667\times10^5$ | $1.125\times10^5$ | $1.300\times10^5$ | $1.143\times10^5$ | $0.727\times10^5$ | $1.8\times10^5$ | $2.0\times10^5$ |
| | $R^2$ | 0.998 | 0.999 | 0.994 | 0.999 | 0.999 | 0.996 | 0.999 | 0.995 | 0.996 | 0.993 |

by acidity. Thus, in order to establish the optimal experimental conditions, we detected the influence of pH value on the binding ability of generating EBBR-SCnA complex utilizing the maximal fluorescence intensity of BR buffer solution ranging from pH 2 to 11 respectively. With the enlargement of their cavity and the changes of pH, the binding constant of EBBR with SCnA shows the certain alterations. As shown in TABLE 2, there is the maximal binding capacity of EBBR with SC4A, SC6A and SC8A when pH value reaches to 6, 7 or 11 respectively. The binding constant of EBBR-SCnA system is relatively low at pH=2. At pH=2, sulfonated calixarenes displays the minimal ionization degree in aqueous solution and the relatively low binding ability, indicating that hydrogen bonds are not their main driving force of the complex system. Regarding to calixarene derivatives, Coleman et al. had also reported that with the increasing pH, the deprotonation of phenolic OH groups of SCnA could be further strengthened, which led to the strengthened hydrogen bonds among the phenolic hydroxyl groups and thus allowed conformation flexibility for the calixarene ring[32]. Because of the property of EBRR as a triple weak acid in EBRR-SCnA system[24], EBBR gradually ionized with the increasing pH, showed the reduced interaction of hydrogen bonding by the outside subject body and thus obtained more ability to enter the subject body through its part of structure. The effect of its size is the other important reason for whose inclusion constants is determined. When pH is low, phenolic hydroxyl on the calixarene is protonated. While pH increases, phenolic hydroxyl group gets deprotonated, phenolic hydroxyl group $O^-$ mutual repulsion from its lower edge leads to a cavity with smaller size, but the cavity of SC4A, SC6A or SC8A gradually increases. Therefore, the optimal cavity for EBBR appears under different pH conditions. Overall, the hydrophobic interaction and size-matched effect are the main reasons that the binding of SCnA to EBBR may be affected. Thus, for SC4A, SC6A and SC8A, BR buffer solution with pH value of 6, 7 and 11 was selected as the corresponding condition for the subsequent experiments.

## The effect of species ions on the determination of EBBR

In this study, the effect of some ions in BR buffer and some wastewater with common dye were examined. The results shows that there is no influence on EBBR-SCnA system when $K^+$、$Na^+$、$SO_4^{2-}$、$CH_3COO^-$、$Cl^-$、$NH_4^+$、$Br^-$、$CO_3^{2-}$、$PO_4^{3-}$、$HPO_4^{2-}$ $0H_2PO_4^-$ as added with 0.1mol $L^{-1}$ concentrations (about 3000 times more than the concentration of samples). So the present study also provides for a possible new method for EBBR detection under different pH and a potential new fluorescent probes for the test of other drugs without fluorescence.

## $^1$H NMR study and molecular modeling calculation

The $^1$H NMR spectra of the formation of a EBBR-SCnA complex is shown in Figure 10(c→e). Compared with proton resonances of the unbound EBBR molecules (Figure 10a), all of H signals protons of the bound EBBR significantly shift. For EBBR-SC4A and EBBR-SC6A (Figure 10c, 10d),

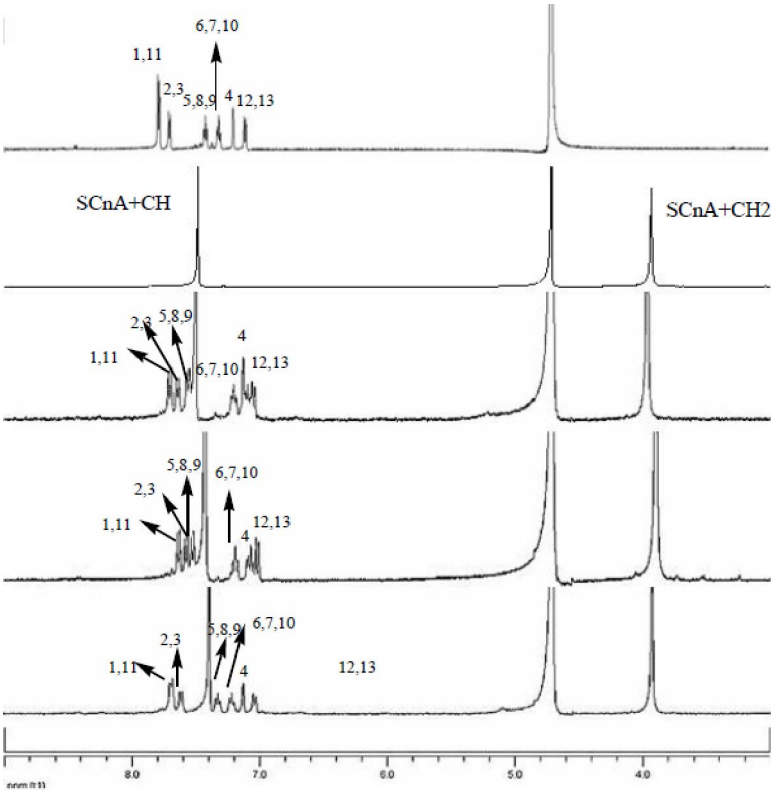


**Figure 10 : $^1$H NMR spectra (600 MHz) of EBBR(a), SC*n*A (b), SC4A-EBBR complex (c), SC6A -EBBR complex (d), and SC8A-EBBR complex (e) in $D_2O$**

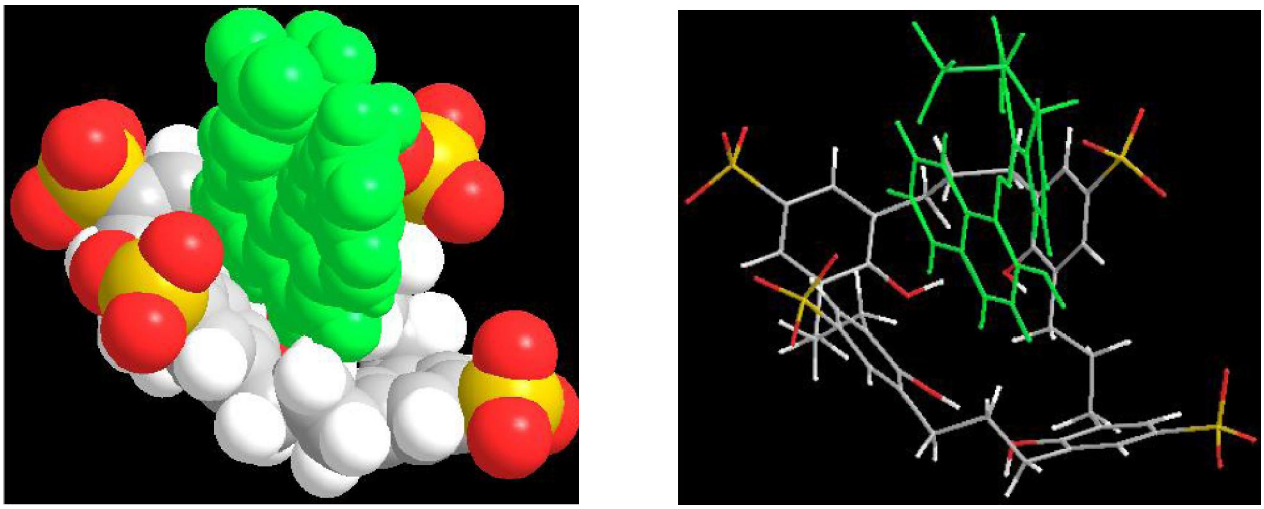

**Figure 11 : Energy-minimized structure of SC*4*A-EBBR complexes in the ground state using balls and tubes for the rendering of atoms. Color codes: EBBR, green; SC*4*A, sulfur, yellow; oxygen, red; carbon, gray; hydrogen, white; lone-pair electron, powder**

only H5 shift toward lowfield while the other H signals protons obviously move upfield and displacement values become bigger with the increasing number of calixarene ring phenol. For EBBR-SC8A (Figure 10e), all of H proton signal clearly move upfield. These findings indicate that under the size-matching condition, a part of the EBBR molecules enters the hydrophobic cavity of sulfonated aromatic to form the inclusion complexes through hydrophobic interactions, which may lead to the shield of the EBBR protons and further fluorescence quenching. With the increasing number of phenolic units of the calixarene ring, the interaction becomes much stronger and the molecular distance gets much closer. These results

are consistent with the above discussion.

Molecular modeling calculations were optimized at the B3LYP/6-31G(d) level of the density functional theory using Gaussian 03 program. Our results confirmed the partial inclusion of EBBR in the upper rim of SCnA. For example, molecular modeling simulation of SC4A-EBBR was performed to obtain the optimized conformation of the host-guest complex (Figure 11). In the energy-minimized structure, Naphthalene ring of EBBR enters partly into the hydrophobic cavity of SC4A and phenolic hydroxyl on naphthalene ring and phenolic hydroxyl on SC4A form weak hydrogen bonds. The conformation was evidenced by the NMR spectra, which is consistent with the previous discussion that their interaction is mainly drived by the hydrophobic interaction and the size-matched effects of the macrocycle.

## CONCLUSION

The inclusion behavior of SCnA with EBBR was studied by fluorescence spectroscopy. 1:1 inclusion stoichiometry and the association constant of the inclusion complex at 20°C were evaluated. The fluorescence intensity of the EBBR guest molecule gradually decreased upon the addition of SCnA(n=4,6,8). The quenching of fluorescence and the stability constant of complex monotonically increased with the growing number of phenolic units in the calixarene ring. The changes of negative free energy have demonstrated that this process was spontaneous. The influence of ionic strength0$^{1}$H NMR study and calculation from molecular modeling showed that hydrophobic interactions and structural matching effect were thought to play main roles in the formation of the host–guest complex. These results expand the application of sulfonated calix[n]arenes in molecular recognition scopes. This method can be used to make a fluoscence probe and a fluorescence sensor for the detection of non-fluorescent or weakly fluorescent substances. Related studies are in progress in our laboratory.

## ACKNOWLEDGEMENTS

This work was supported by the National Natural Science Foundation of China (No. 21171110) and the Research Fund for the Doctoral Program of Higher Education of China (No.20091404110001). Helpful suggestions by anonymous referees are also gratefully acknowledged.

## REFERENCES

**[1]** J.Song, H.Li, J.Chao, C.Dong, S.Shuang; Journal of inclusion phenomena and macrocyclic chemistry, **72**, 389-395 **(2012)**.

**[2]** M.Bayrakcý, A.N.Kursunlu, E.Güler, [a].Ertul; Dyes and Pigments, **99**, 268-274 **(2013)**.

**[3]** V.Böhmer; Angewandte chemie international edition in english, **34**, 713-745 **(1995)**.

**[4]** J.Chao, Y.Zhang, X.Fan, H.Wang, Y.Li; Spectrochimica Acta Part A: Molecular and Biomolecular Spectroscopy, **116**, 295-300 **(2013)**.

**[5]** M.Snejdarkova, A.Poturnayova, P.Rybar, P.Lhotak, M.Himl, K.Flidrova, T.Hianik; Bioelectrochemistry, **80**, 55-61 **(2010)**.

**[6]** W.Y.Li, H.Li, G.M.Zhang, J.B.Chao, L.X.Ling, S.M.Shuang, C.Dong; Journal of Photochemistry and Photobiology A: Chemistry, **197**, 389-393 **(2008)**.

**[7]** J.Millership; Journal of Inclusion Phenomena and Macrocyclic Chemistry, **39**, 327-331 **(2001)**.

**[8]** F.Perret, A.N.Lazar, A.W.Coleman; Chem.Commun., DOI: 10.1039/B600720C, 2425-2438 **(2006)**.

**[9]** D.Cuc, S.Bouguet-Bonnet, N.Morel-Desrosiers, J.P.Morel, P.Mutzenhardt, D.Canet; The Journal of Physical Chemistry B, **113**, 10800-10807 **(2009)**.

**[10]** C.Chen, J.F.Ma, B.Liu, J.Yang, Y.Y.Liu; Crystal Growth & Design, **11**, 4491-4497 **(2011)**.

**[11]** G.Arena, A.Contino, F.Giuseppe Gulino, A.Magrì, F.Sansone, D.Sciotto, R.Ungaro; Tetrahedron Lett., **40**, 1597-1600 **(1999)**.

**[12]** G.Arena, A.Casnati, A.Contino, F.G.Gulino, D.Sciotto, R.Ungaro; Journal of the Chemical Society, Perkin Transactions 2, DOI: 10.1039/A909847J, 419-423 **(2000)**.

**[13]** G.Arena, A.Contino, F.G.Gulino, A.MagrýÌ, D.Sciotto, R.Ungaro; Tetrahedron Lett., **41**, 9327-9330 **(2000)**.

**[14]** Y.Liu, B.H.Han, Y.T.Chen; The Journal of Organic Chemistry, **65**, 6227-6230 **(2000)**.

**[15]** W.Tao, M.Barra; The Journal of Organic Chemistry, **66**, 2158-2160 **(2001)**.

**[16]** L.Memmi, A.Lazar, A.Brioude, V.Ball, A.W.Coleman; Chem.Commun., DOI: 10.1039/B109190P, 2474-2475 **(2001)**.
**[17]** H.Li, J.P.Song, J.B.Chao, S.M.Shuang, C.Dong; Spectrochimica Acta Part A: Molecular and Biomolecular Spectroscopy, **97**, 155-160 **(2012)**.
**[18]** Y.Zhou, Q.Lu, C.Liu, S.She, L.Wang; Spectrochimica Acta Part A: Molecular and Biomolecular Spectroscopy, **64**, 748-756 **(2006)**.
**[19]** M.Megyesi, L.Biczókl; Chem.Phys.Lett., **424**, 71-76 **(2006)**.
**[20]** L.Ma, X.Zhu; Spectrochimica Acta Part A: Molecular and Biomolecular Spectroscopy, **95**, 246-251 **(2012)**.
**[21]** H.W.Gao; Recl.Trav.Chim.Pays-Bas, **114**, 61-64 **(1995)**.
**[22]** J.F.Zhao, S.Q.Xia, H.W.Gao, Y.L.Zhang; Instrumentation Science & Technology, **32**, 77-91 **(2004)**.
**[23]** Y.Zhao, W.Chang, Y.Ci, Talanta; **59**, 477-484 **(2003)**.
**[24]** S.Pirillo, M.L.Ferreira, E.H.Rueda; J.Hazard.Mater., **168**, 168-178 **(2009)**.
**[25]** C.F.Li, L.M.Du, H.M.Zhang; Spectrochimica Acta Part A: Molecular and Biomolecular Spectroscopy, **75**, 912-917 **(2010)**.
**[26]** H.Wang, R.Cao, C.F.Ke, Y.Liu, T.Wada, Y.Inoue; The Journal of Organic Chemistry, **70**, 8703-8711 **(2005)**.
**[27]** Y.J.Hu, Y.Liu, X.S.Shen, X.Y.Fang, S.S.Qu; J.Mol.Struct., **738**, 143-147 **(2005)**.
**[28]** C.Bonal, Y.Israeli, J.P.Morel, N.Morel-Desrosiers; Journal of the Chemical Society, Perkin Transactions 2, DOI: 10.1039/B102038M, 1075-1078 **(2001)**.
**[29]** W.Tao, M.Barra; Journal of the chemical society, Perkin transactions 2, DOI: 10.1039/A802841I, 1957-1960 **(1998)**.
**[30]** Y.Zhou, H.Xu, L.Wu, C.Liu, Q.Lu, L.Wang; Spectrochimica acta part A: molecular and biomolecular spectroscopy, **71**, 597-602 **(2008)**.
**[31]** X.P.Ding, D.B.Tang, T.Li, S.F.Wang, Y.Y.Zhou; Spectrochimica acta part a: Molecular and Biomolecular Spectroscopy, **81**, 44-47 **(2011)**.
**[32]** A.W.Coleman, S.G.Bott, S.D.Morley, C.M.Means, K.D.Robinson, H.Zhang, J.L.Atwood; Angewandte Chemie International Edition in English, **27**, 1361-1362 **(1988)**.